Published in final edited form as:
Nature. 2007 November 15; 450(7168): 370–375. doi:10.1038/nature06266.

Portability of paddle motif function and pharmacology in voltage sensors

AbdulRasheed A. Alabi[1,†], **Maria Isabel Bahamonde**[1,†], **Hoi Jong Jung**[2], **Jae Il Kim**[2], and **Kenton J. Swartz**[1]

[1]Molecular Physiology and Biophysics Section, Porter Neuroscience Research Center, National Institute of Neurological Disorders and Stroke, National Institutes of Health, Bethesda, MD 20892 USA

[2]Department of Life Sciences, Gwangju Institute of Science and Technology, Gwangju, 500-712 Korea

Abstract

Voltage-sensing domains enable membrane proteins to sense and react to changes in membrane voltage. Although identifiable S1–S4 voltage-sensing domains are found in an array of conventional ion channels and in other membrane proteins that lack pore domains, the extent to which their voltage sensing mechanisms are conserved is unknown. Here we show that the voltage-sensor paddle, a motif composed of S3b and S4 helices, can drive channel opening with membrane depolarization when transplanted from an archaebacterial voltage-activated potassium (Kv) channel (KvAP) or voltage-sensing domain proteins (Hv1 and Ci-VSP) into eukaryotic Kv channels. Tarantula toxins that partition into membranes can interact with these paddle motifs at the protein-lipid interface and similarly perturb voltage sensor activation in both ion channels and voltage-sensing domain proteins. Our results show that paddle motifs are modular, that their functions are conserved in voltage sensors, and that they move in the relatively unconstrained environment of the lipid membrane. The widespread targeting of voltage-sensor paddles by toxins demonstrates that this modular structural motif is an important pharmacological target.

Ion channels that open and close in response to changes in membrane voltage have a modular architecture, with a central pore domain that determines ion selectivity, and four surrounding voltage sensing domains that move in response to changes in membrane voltage to drive opening of the pore [1–5] (Fig 1a). Although X-ray structures have now been solved for two voltage-activated potassium (Kv) channels [1, 6–9], the structural basis of voltage sensing remains controversial [10–12]. A seminal observation in the X-ray structures of the KvAP channel, an archaebacterial Kv channel from *Aeropyrum pernix*, was that the S3b helix and the charge-bearing S4 helix within the voltage-sensing domain form a helix-turn-helix structure, termed the paddle motif [1, 8, 9]. Studies on KvAP [1, 9, 13–16] suggest that this voltage-sensor paddle is buried in the membrane and that it moves at the protein-lipid interface, which contrasts with models for eukaryotic Kv channels where the S4 helix is protected from membrane lipids by other regions of the protein [10–12, 17–21]. Voltage-sensing domains have also recently been described in voltage-sensing proteins that lack associated pore domains [5, 22, 23]. In Ci-VSP the voltage-sensing domain is coupled to a phosphatase domain and in Hv1 the voltage-sensing domain itself is thought to function as a proton channel. Here we explore whether the mechanisms of voltage-sensing are conserved between the distantly related eukaryotic and

Correspondence to: Kenton J. Swartz.

†These authors contributed equally

Competing interest statement

The authors declare that they have no competing interest

archaebacterial Kv channels, and the newly discovered voltage-sensing domain proteins, Ci-VSP and Hv1. Using a chimera approach, we first examine whether specific structural elements within voltage sensors can be transferred between Kv channels and voltage-sensing domain proteins while preserving functional responses to changes in membrane voltage. We then use a family of tarantula toxins that interact with voltage-sensing domains to explore the structural integrity of these modular motifs and their disposition with respect to the lipid membrane.

Chimeras between Kv channels

We began by generating chimeras between the archaebacterial KvAP channel [24] and the eukaryotic Kv2.1 channel from rat brain [25] to define the interchangeable regions. Transfer of the KvAP pore domain into Kv2.1 results in channels that open in response to membrane depolarization (Fig 1a; Supplementary Fig 1 and Table 1), so long as the S4–S5 linker helix and the most C-terminal region of the S6 helix are from the same channel, a result that reaffirms the modular architecture of Kv channels and the important roles of the S4–S5 and S6 helices in coupling the voltage-sensing and pore domains [4, 26]. We then turned to identifying those regions within the voltage-sensing domains that are compatible, and in doing so produced > 60 chimeras that varied in the amount of KvAP sequence they contained and the region transferred (Fig 1; Supplementary Fig 1). The vast majority of these constructs result in non-functional channels (Fig 1a; Supplementary Fig 1), a result that is not surprising given that these constructs typically contain many (often radical) amino acid changes. One region stands out, however, where relatively large portions of KvAP can be transferred into Kv2.1 without disrupting channel function. The transferable region begins at the junction between S3a and S3b helices and ends just past the first four critical Arg residues in S4 [17, 27, 28], corresponding to the paddle motif identified in the X-ray structure of KvAP [1] (Fig 1a–d). These paddle chimeras display robust voltage-activated K^+ currents and gating properties that are qualitatively similar to Kv2.1 (Fig 1d). A similar chimera where the paddle of KvAP is transferred to the Shaker Kv channel from *Drosophila* [29] also results in functional Kv channels (Fig 2a; Supplementary Table 1), suggesting that the results with Kv2.1 are applicable to other types of Kv channels. Extending the region transferred by extension on the N-terminal side of the paddle into the S3a helix or on the C-terminal side beyond the first four Arg residues in S4 results in non-functional channels (Fig 1b, Supplementary Fig 1). The inability to extend into the C-terminal portion of S4 is consistent with the presence of crucial protein-protein interactions between the inner regions of the S4 and S5 helices [30]. The preservation of channel function observed in the paddle chimeras is quite remarkable considering the large number of amino acid substitutions they contain. One such chimera (C7[S3–S4]AP) contains 25 residue substitutions (15 of which are non-conservative) and a 7-residue deletion. In the context of so many chimeras that do not result in functional channels, the successful transfer of the paddle motif suggests that this region is modular and unique in its paucity of rigidly constraining side chain interactions with other parts of the protein.

Tarantula toxins interacting with paddle motifs in Kv channels

To further explore the structural and functional integrity of the chimeras, we examined their sensitivities to tarantula toxins known to inhibit Kv channels by interacting with voltage sensors. The two toxins we focused on are hanatoxin (HaTx), which does not interact with KvAP, but inhibits Kv2.1 by interacting with its voltage-sensor paddle [31–37], and VSTx1, a related tarantula toxin that does not inhibit either Kv2.1 or Shaker (Fig 2a), but inhibits KvAP by binding somewhere within its S1–0S4 domain [9, 24, 38]. Transferring the KvAP paddle into Shaker (C*[S3–S4]AP) renders this eukaryotic Kv channel sensitive to extracellular VSTx1 (Fig 2a), suggesting that this tarantula toxin interacts with the paddle motif in KvAP, similar to the interaction of HaTx with the Kv2.1 channel. Transferring the S3b helix of KvAP alone into Kv2.1 (C3[S3]AP) results in a channel that is insensitive to extracellular HaTx (Fig 2a),

which makes sense because KvAP is insensitive to HaTx and the most crucial determinants of HaTx binding to Kv2.1 are localized within S3b [31–37]. In the case of VSTx1, transferring the S4 helix alone from KvAP into Kv2.1 (C2[S4]AP, C4[S4]AP, C9[S4]AP) is sufficient to render the recipient channel sensitive to VSTx1, in each case without disrupting sensitivity to HaTx (Fig 2a). Although these results do not preclude important interactions between VSTx1 and the S3b helix of the paddle, they point to a particularly important role of the S4 helix.

One of the hallmarks of toxins that inhibit by stabilizing the resting state of the paddle motif (e.g. HaTx) is that inhibition can be overcome when the channel is activated with strong depolarization of the membrane [31, 35, 36]. Although VSTx1 prevents opening of chimeras containing the S4 helix from KvAP in the Kv2.1 channel (e.g. C2[S4]AP) when activating the channel using weak depolarizations to 0 mV, the channel opens robustly in response to large depolarizations to +60 mV (Fig 2b). In effect, VSTx1 shifts activation of the channel to more depolarized voltages (Fig 2c), similar to what is seen in the case of HaTx [31, 35, 36]. Similar shifts of channel activation are observed for each of the VSTx1-sensitive paddle chimeras studied here (data not shown). The kinetics of channel activation are biphasic in the presence of VSTx1 (Fig 2b), raising the possibility that the toxin unbinds during strong depolarizations, an inference that is supported by experiments using multiple pulse protocols to measure toxin dissociation (Supplementary Fig 2). Taken together, these results suggest that tarantula toxins interact with helices in the voltage-sensor paddle motif and that these interactions are appropriately preserved in the chimeras. Both of these toxins are thought to interact with their target channels within the lipid membrane [14, 36, 37, 39, 40], which fits nicely with the portability of the paddle between the two types of distantly related Kv channels because it suggests that the unconstrained environment is actually the lipid membrane.

Structural analysis of the tarantula toxin-paddle interaction

Although it is clear that the paddle motif is the receptor for tarantula toxins like HaTx in Kv2.1 [31–37], the disposition of the toxin-binding surface with respect to the lipid membrane and other regions of the protein is unclear. HaTx does not interact tightly with either KvAP or Kv1.2, the two Kv channels for which X-ray structures are available, and the sequence similarity between these channels and Kv2.1 is quite low, precluding assignment of crucial residues within the existing structures. The interaction of VSTx1 with chimeras containing the entire paddle of KvAP (Fig 2), however, offers an opportunity to explore the structure of a tarantula toxin receptor because there are three X-ray structures of KvAP [1, 8], and the structure of the paddle motif in these is very similar (whether or not an antibody is bound). To define critical residues within the paddle motif that may interact with VSTx1, we Ala scanned the paddle region of the C*[S3–S4]AP chimera between KvAP and Shaker. Most of the 29 residues within the KvAP paddle in this construct were individually mutated to Ala (except for native alanines which were mutated to Val), and the effects on the apparent affinity of the toxin determined [31–37]. Ten mutants stand out as having dramatic effects on toxin sensitivity, including L102A, L105A, I106A, G108A and H109A within the S3b helix, G114A and L115A within the connecting loop, and then L118A, L122A and L125A within the S4 helix (Fig 3a; Supplementary Table 2). When mapped onto the high resolution structure of the isolated voltage-sensing domain of KvAP [1], the results provide a remarkable picture of how the toxin must dock onto the paddle motif because with the exception of G108A, all of the crucial side chains are located on a contiguous surface of the S3b–S4 helix-turn-helix motif (Fig 3b). This surface is striking in that it is largely comprised of the aliphatic residues Ile and Leu, with H109 being the single important polar residue. We can see the disposition of this surface with respect to the rest of the channel and the surrounding lipid membrane by positioning the voltage-sensing domain of KvAP relative to the pore domain in a fashion that is consistent with the X-ray structure of Kv1.2 [7] (Fig 3c). The surface of the paddle that is critical for interacting with VSTx1 projects out towards the surrounding lipid bilayer, revealing that the toxin docks onto

the paddle motif at the perimeter of the channel. This structural picture is consistent with functional studies suggesting that tarantula toxins interact with Kv channels within the lipid bilayer [14, 36, 37, 39, 40], and that multiple toxins (perhaps up to 4) can bind to a single Kv channel relatively independently [31, 35]. The intimate involvement of membrane lipids in contributing to the toxin receptor [40] is also supported by these mutagenesis results because non-annular lipids that have been resolved in crystal structures [41] often intercalate between the types of aliphatic residues dominating the surface of the paddle that is crucial for toxin binding.

Chimeras between voltage-sensing proteins and Kv channels

Although the recently discovered voltage-sensing proteins, Ci-VSP and Hv1 [5, 22, 23], contain recognizable S1–S4 transmembrane segments, the relationship between their voltage-sensing domains and those found in ion channels has yet to be explored. Emboldened by the successful transfer of paddle motifs between KvAP and eukaryotic Kv channels, we examined whether similar regions of the voltage-sensing proteins can drive opening of eukaryotic Kv channels. We constructed a series of chimeras by transferring regions of the voltage-sensing domains of Ci-VSP and Hv1 into Kv2.1, and similar to our results with KvAP, discovered that the paddle region of these voltage-sensing proteins is competent to drive opening of the eukaryotic Kv channel (Fig 4a–c). Robust voltage-activated K^+ currents are observed for several chimeras containing the paddle region of the voltage-sensing proteins, but extension of these constructs to include larger regions of the voltage-sensing domains does not result in functional channels (Supplementary Fig 4 and Table 3). These results reinforce the notion that the paddle motif moves in a relatively unconstrained environment and suggest that the general mechanisms of voltage-sensing are similar between Kv channels and voltage-sensing domain proteins.

Tarantula toxins interacting with paddle motifs from voltage-sensing proteins

To explore whether tarantula toxins can interact with the paddle motifs of voltage-sensing domain proteins, we tested the activity of five tarantula toxins and crude *Grammostola spatulata* venom on chimeras containing paddles from Hv1 or Ci-VSP in the Kv2.1 channel. Remarkably, HaTx, GmTxSIA [3, 42] and crude venom inhibit the Hv1 paddle chimera by shifting activation to positive voltages (Fig 5a), similar to what is seen for the interaction of tarantula toxins with Kv channels [37]. To confirm that HaTx interacts with the paddle region of Hv1, we mutated several residues within the transferred region and find that the D185A mutant effectively eliminates the inhibitory effects of the toxin (Supplementary Fig 5). To examine whether the interaction between HaTx and the Hv1 paddle in the chimera is predictive of interactions between the toxin and the Wt Hv1 protein, we expressed Hv1 alone and tested whether HaTx can inhibit voltage-activated proton currents. Extracellular application of HaTx produces robust inhibition of Hv1 proton currents (Fig 5b), revealing that the toxin can interact with the voltage-sensing domain of the Hv1 protein itself. When examined over a range of membrane voltages, we observe that HaTx shifts activation of the Hv1 protein to more positive voltages (Fig 5b–c). Taken together, these results suggest that tarantula toxins can interact with paddle motifs regardless of whether they are present in Kv channels or voltage-sensing domain proteins. Although HaTx, SGTx1 [43], VSTx1[24], GmTxSIA and GxTx1E [44] have little effect on the activity of the Ci-VSP chimera, the crude venom contains clear inhibitory activity (see Supplementary Fig 6). All of the toxins thus far isolated from *Grammostola spatulata* venom are related to HaTx and VSTx1 [37], raising the possibility that tarantula venom contains a related toxin that targets the paddle motif of Ci-VSP.

Conclusions

The present results with paddle chimeras and tarantula toxins have three general implications for the structural basis of voltage sensing. First, they suggest that the paddle motif is a modular unit common to voltage sensors, whether they are found in eukaryotic or archaebacterial Kv channels, or voltage-sensing proteins like the Ci-VSP voltage-sensitive phosphatase or the Hv1 voltage-gated proton channel. The ability of the paddle to support both voltage and toxin sensitivity argues that the fundamental voltage sensing mechanism is likely conserved between these distantly related membrane proteins. Second, the portability of the paddle motif amongst voltage sensors with low sequence similarity suggests that this motif resides in a relatively unconstrained environment. In order to successfully transplant such dissimilar paddle motifs in the context of extensive packing with the surrounding protein, one would have to transplant all interacting regions. The ability of tarantula toxins to interact with the paddle within the membrane [14, 36, 37, 39, 40], as well as the projection of residues important for toxin binding out towards the surrounding lipid membrane (Fig 3), strongly suggests that the lipid membrane is the flexible environment surrounding the paddle motif. Our results do not preclude crucial side chain interactions between a small subset of residues in the paddle and other parts of the voltage sensor. The charge carrying Arg residues, for example, are thought to interact with acidic residues in S2 and S3 [28, 45], and there appears to be specificity in the positions in S4 where charged moieties contribute to the total gating charge [17]. The Arg residues are the most conserved positions in our paddle constructs, so important interactions involving these residues are fully compatible with our results. Third, the picture of tarantula toxins interacting with crucial residues in both S3b and S4 (Fig 2, Fig 3), when taken together with the fact that the paddle can move with the toxin continuously bound [36] (Supplementary Fig 2), suggest that these two helices within the paddle move roughly as a unit in response to changes in membrane voltage. Large rotations of the S4 helix relative to S3b [18], for example, would be hard to reconcile with the present picture of tarantula toxins docking onto the paddle motif (Fig 3).

The demonstration that paddle motifs are portable modules also has exciting implications for studying proteins that contain voltage sensors because it means that new proteins can be engineered with specific paddle motifs that are tailored for a particular purpose. We used the modular feature of voltage-sensor paddles to screen paddles from voltage-sensing domain proteins for interactions with tarantula toxins using Kv channel activity as an assay, which could be adapted for high-throughput screening of chemical libraries for compounds that interact with paddle motifs from any protein that contains a voltage sensor. X-ray structures are available for only KvAP and Kv1.2 channels [1, 7, 8], and in each of these structures there are key regions that are poorly defined or distorted. MacKinnon and colleagues use the portability of the paddle motif to solve a new X-ray structure of a Kv channel with a paddle variant [46], leading to important new insights into the structural basis of voltage sensing.

Previous studies on the interaction of HaTx with voltage sensors in Kv2.1 channels suggest that the paddle motif observed in the KvAP X-ray structure is the key region of the channel that the toxin targets [3, 31–37, 43]. The present studies with tarantula toxins that interact with paddle motifs in a wide range of distantly related proteins with voltage sensors, including KvAP, Ci-VSP and Hv1 (Fig 6), establish the general principle that the modular paddle motif is an important pharmacological target. VSTx1 interacts with the paddle motif in KvAP, HaTx can recognize the paddle motif in either Hv1 or Kv2.1, and other toxins in tarantula venom likely interact with the paddle of the voltage-sensitive phosphatase. It will be fascinating to use these emerging ideas about paddle motifs to identify new molecules and drugs that modulate the activity of the large and diverse variety of membrane proteins that contain voltage-sensing domains. It will also be exciting to explore the possibility that ion channels only distantly related to Kv channels, for example Transient Receptor Potential (TRP) channels, will contain paddle-like motifs that have related roles in channel gating and represent important

pharmacological targets. Indeed, several recently discovered tarantula toxins that are strikingly similar to those studied here, have been shown to activate the capsaicin receptor channel, TRPV1 [47]. It appears that nature has targeted the paddle throughout evolution, with tarantulas being just one example of the organisms that produce paddle toxins [37]. Such widespread targeting of the paddle motif can be explained by the observation that this modular structural motif is a uniquely mobile region within S1–S4 voltage-sensing domains [13].

Methods Summary

Chimeras and point mutations were generated using either KvAP [24], Ci-VSP [5], Hv1[23], Kv2.1Δ7 [3, 25] or Shaker H4 [29]. Most channel constructs were expressed in *Xenopus* oocytes [35] and studied using two-electrode voltage clamp recording techniques. For most experiments the external recording solution contained (in mM): 50 KCl, 50 NaCl, 10–20 HEPES, 1 $MgCl_2$, 0.3 $CaCl_2$, pH 7.4–7.6. For the C*[S3–S4]AP chimera, the external solution contained (in mM): 4 KCl, 96 NaCl, 10 HEPES, 1 $MgCl_2$, 0.3 $CaCl_2$, pH 7.6. Macroscopic proton currents were recorded in whole-cell mode using a patch-clamp amplifier. The intracellular (pipette) solution contained (in mM): 100 Bis-Tris, 75 NaCl, 1 EGTA, 2 $MgCl_2$, pH 6.5 and the extracellular (bath) solution contained (in mM): 100 Bis-Tris, 75 NaCl, 1 EGTA, 3 $CaCl_2$, pH 6.5. Hanatoxin was purified from *Grammostola spatulata* venom [48]. VSTx1, SGTx1 and GxTx1E were synthesized using solid phase chemical methods, folded and purified, as previously described [39, 43]. GmTxSIA was generously provided by Richard A. Keith and Richard A. Lampe, (Zeneca Inc.). Voltage-activation relations for all constructs were obtained by measuring tail currents following a series of membrane depolarizations or by measuring steady-steady state currents and calculating conductance. Occupancy of closed/resting channels by tarantula toxins was examined using negative holding voltages where open probability is very low, and the fraction of unbound channels (F_u) was estimated using depolarizations that are too weak to open toxin-bound channels, as previously described [3, 31–37, 43] (Supplementary Fig 3). Example traces showing the inhibitory activity of tarantula toxins were taken for relatively weak depolarizations for that particular channel construct. The apparent equilibrium dissociation constant (K_d) was calculated assuming four independent toxin binding sites per channel with single occupancy being sufficient to inhibit opening in response to weak depolarizations.

$$K_d=((1/(1-F_u^{1/4}))-1)[\text{Toxin}]$$

Full Methods and any associated references are available in the online version of the paper at www.nature.com/nature.

METHODS

Channel and chimera constructs

Chimeras and point mutations were generated using sequential polymerase chain reactions (PCR) with either KvAP [24], Ci-VSP [5], Hv1[23], Kv2.1Δ7 [3, 25] or Shaker H4 [29] as templates. The Kv2.1 Δ7 construct contains 7 point mutations in the outer vestibule [3], rendering the channel sensitive to agitoxin-2, a pore blocking toxin from scorpion venom [49], and the Shaker construct contains a deletion of residues 6 through 46 to remove fast inactivation [50]. KvAP was amplified from *Aeropyrum pernix* genomic DNA (ATCC Inc.) and human Hv1 was amplified from clone NIH-MGC-92 (ID: 5577070; NIH Mammalian Gene Collection; Invitrogen). The DNA sequence of all constructs was confirmed by automated DNA sequencing and cRNA was synthesized using T7 polymerase after linearizing DNA with appropriate restriction enzymes.

Two-electrode voltage clamp recording from *Xenopus* oocytes—Channel constructs were expressed in *Xenopus* oocytes [35] and studied using two-electrode voltage clamp recording techniques (OC-725C; Warner Instruments) with a 200 µl recording chamber. For most experiments the external recording solution contained (in mM): 50 KCl, 50 NaCl, 10–20 HEPES, 1 $MgCl_2$, 0.3 $CaCl_2$, pH 7.4–7.6 with NaOH. In order to record outward tail currents for the C*[S3–S4]AP chimera, the external solution contained (in mM): 4 KCl, 96 NaCl, 10 HEPES, 1 $MgCl_2$, 0.3 $CaCl_2$, pH 7.6 with NaOH. Data were filtered at 2 kHz and digitized at 10 kHz. Microelectrode resistances were 0.1–1 MΩ when filled with 3M KCl. All experiments were performed at room temperature (~22 ºC). One technical difficulty in studying the toxin sensitivity of chimeras containing the entire KvAP paddle in Kv2.1 (C7[S3–S4]AP) is that these constructs display pronounced sensitivity to silver released from bath ground wires, resulting in pronounced inhibition when the flow of solution around the oocyte is stopped (for conserving the quantities of toxins used in experiments). We therefore limited our study of toxin-channel interactions to the chimera containing the KvAP paddle in Shaker (C*[S3–S4)] AP), or chimeras containing parts of the KvAP paddle in Kv2.1, constructs for which this technical problem is not pronounced. Leak and background conductances, identified by blocking the channel with agitoxin-2 [49], have been subtracted for all of the Kv channel currents shown[35].

Patch recording from HEK cells

Macroscopic proton currents were recorded in whole-cell mode using a patch-clamp amplifier (Axopatch 200B). Data were filtered at 1 or 2 kHz (8-pole Bessel) and digitized at 20 kHz. Patch pipette resistance when filled with the recording solution was 1–2 MΩ. The intracellular (pipette) solution contained (in mM): 100 Bis-Tris, 75 NaCl, 1 EGTA, 2 $MgCl_2$, pH 6.5 and the extracellular (bath) solution contained (in mM): 100 Bis-Tris, 75 NaCl, 1 EGTA, 3 $CaCl_2$, pH 6.5. When activating the Hv1 channel with voltage steps that are long enough to reach steady state (~2 to 3 sec), the resulting proton currents were somewhat unstable when examined with repeated pulses to the same voltage, a phenomenon that we attribute to proton depletion near the membrane. To circumvent this problem we limited the pulse duration to 1.5 sec, pulse frequency to 0.05 Hz and studied cells with moderate expression levels, manipulations that result in relatively stable and reproducible proton currents. All experiments were performed at room temperature (~22 °C).

Toxin purification and synthesis

Hanatoxin was purified from *Grammostola spatulata* venom (Spider Pharm) as previously described [48]. VSTx1, SGTx1 and GxTx1E were synthesized using solid phase chemical methods, folded and purified, as previously described [39, 43]. GmTxSIA was generously provided by Richard A. Keith and Richard A. Lampe, (Zeneca Inc.).

Analysis of channel activity and toxin-channel interactions

Voltage-activation relations were obtained by measuring tail currents or steady-state currents (and calculating conductance), and a single Boltzmann function was fit to the data according to:

$$I/I_{max}=(1+e^{-zF(V-V_{1/2})/RT})^{-1}$$

where I/I_{max} is the normalized tail current amplitude, z is the equivalent charge, $V_{1/2}$ is the half-activation voltage, F is Faraday's constant, R is the gas constant and T is temperature in Kelvin.

Occupancy of closed/resting channels by tarantula toxins was examined using negative holding voltages where open probability is very low, and the fraction of unbound channels (F_u) was estimated using depolarizations that are too weak to open toxin-bound channels, as previously described [3, 31–37, 43] (Supplementary Fig 3). Because toxin-bound channels close or deactivate more rapidly than unbound channels, we examined the kinetics of deactivation using tail currents to confirm that toxin-bound channels did not contribute to the currents measured with weak depolarizations. After addition of the toxin to the recording chamber, the equilibration between toxin and channel was monitored using weak depolarizations elicited at 4 to 20 sec intervals. For all channels, we recorded voltage-activation relations (typically from tail currents) in the absence and presence of different concentrations of toxin. The ratio of currents (I/I_0) recorded in the presence (I) and absence of toxin (I_0) was calculated for various strength depolarizations, typically −70 to +90 mV. The value of I/I_0 measured in the plateau phase at voltages where toxin-bound channels do not open [3, 31–37, 43] was taken as F_u (see Supplementary Fig 3 as an example). The apparent equilibrium dissociation constant (K_d) was calculated assuming four independent toxin binding sites per channel with single occupancy being sufficient to inhibit opening in response to weak depolarizations.

$$K_d=((1/(1-F_u^{1/4}))-1)[\text{Toxin}]$$

For all chimeras and mutants, voltage protocols were adjusted appropriately so that the plateau phase in the I/I_0-voltage relation was well-defined (see Supplementary Figure 3). Example traces showing the inhibitory activity of tarantula toxins were taken for relatively weak depolarizations within the plateau phase for that particular channel construct.

Supplementary Material

Refer to Web version on PubMed Central for supplementary material.

References

1. Jiang Y, et al. X-ray structure of a voltage-dependent K+ channel. Nature 2003;423:33–41. [PubMed: 12721618]
2. Kubo Y, Baldwin TJ, Jan YN, Jan LY. Primary structure and functional expression of a mouse inward rectifier potassium channel. Nature 1993;362:127–133. [PubMed: 7680768]
3. Li-Smerin Y, Swartz KJ. Gating modifier toxins reveal a conserved structural motif in voltage- gated Ca2+ and K+ channels. Proc Natl Acad Sci U S A 1998;95:8585–8589. [PubMed: 9671721]
4. Lu Z, Klem AM, Ramu Y. Ion conduction pore is conserved among potassium channels. Nature 2001;413:809–813. [PubMed: 11677598]
5. Murata Y, Iwasaki H, Sasaki M, Inaba K, Okamura Y. Phosphoinositide phosphatase activity coupled to an intrinsic voltage sensor. Nature 2005;435:1239–1243. [PubMed: 15902207]
6. Long SB, Campbell EB, Mackinnon R. Voltage sensor of Kv1.2: structural basis of electromechanical coupling. Science 2005;309:903–908. [PubMed: 16002579]
7. Long SB, Campbell EB, Mackinnon R. Crystal structure of a mammalian voltage-dependent Shaker family K+ channel. Science 2005;309:897–903. [PubMed: 16002581]
8. Lee SY, Lee A, Chen J, Mackinnon R. Structure of the KvAP voltage-dependent K+ channel and its dependence on the lipid membrane. Proc Natl Acad Sci U S A. 2005
9. Jiang Y, Ruta V, Chen J, Lee A, MacKinnon R. The principle of gating charge movement in a voltage-dependent K+ channel. Nature 2003;423:42–48. [PubMed: 12721619]
10. Tombola F, Pathak MM, Isacoff EY. How far will you go to sense voltage? Neuron 2005;48:719–725. [PubMed: 16337910]
11. Ahern CA, Horn R. Stirring up controversy with a voltage sensor paddle. Trends Neurosci 2004;27:303–307. [PubMed: 15165733]

12. Swartz KJ. Towards a structural view of gating in potassium channels. Nat Rev Neurosci 2004;5:905–916. [PubMed: 15550946]
13. Ruta V, Chen J, MacKinnon R. Calibrated measurement of gating-charge arginine displacement in the KvAP voltage-dependent K+ channel. Cell 2005;123:463–475. [PubMed: 16269337]
14. Lee SY, MacKinnon R. A membrane-access mechanism of ion channel inhibition by voltage sensor toxins from spider venom. Nature 2004;430:232–235. [PubMed: 15241419]
15. Schmidt D, Jiang QX, MacKinnon R. Phospholipids and the origin of cationic gating charges in voltage sensors. Nature 2006;444:775–779. [PubMed: 17136096]
16. Cuello LG, Cortes DM, Perozo E. Molecular architecture of the KvAP voltage-dependent K+ channel in a lipid bilayer. Science 2004;306:491–495. [PubMed: 15486302]
17. Ahern CA, Horn R. Specificity of charge-carrying residues in the voltage sensor of potassium channels. J Gen Physiol 2004;123:205–216. [PubMed: 14769847]
18. Campos FV, Chanda B, Roux B, Bezanilla F. Two atomic constraints unambiguously position the S4 segment relative to S1 and S2 segments in the closed state of Shaker K channel. Proc Natl Acad Sci U S A 2007;104:7904–7909. [PubMed: 17470814]
19. Grabe M, Lai HC, Jain M, Nung Jan Y, Yeh Jan L. Structure prediction for the down state of a potassium channel voltage sensor. Nature 2007;445:550–553. [PubMed: 17187053]
20. Tombola F, Pathak MM, Gorostiza P, Isacoff EY. The twisted ion-permeation pathway of a resting voltage-sensing domain. Nature 2007;445:546–549. [PubMed: 17187057]
21. Chanda B, Asamoah OK, Blunck R, Roux B, Bezanilla F. Gating charge displacement in voltage-gated ion channels involves limited transmembrane movement. Nature 2005;436:852–856. [PubMed: 16094369]
22. Sasaki M, Takagi M, Okamura Y. A Voltage Sensor-Domain Protein is a Voltage-Gated Proton Channel. Science 2006;312:589–592. [PubMed: 16556803]
23. Ramsey IS, Moran MM, Chong JA, Clapham DE. A voltage-gated proton-selective channel lacking the pore domain. Nature 2006;440:1213–1216. [PubMed: 16554753]
24. Ruta V, Jiang Y, Lee A, Chen J, MacKinnon R. Functional analysis of an archaebacterial voltage-dependent K+ channel. Nature 2003;422:180–185. [PubMed: 12629550]
25. Frech GC, VanDongen AM, Schuster G, Brown AM, Joho RH. A novel potassium channel with delayed rectifier properties isolated from rat brain by expression cloning. Nature 1989;340:642–645. [PubMed: 2770868]
26. Lu Z, Klem AM, Ramu Y. Coupling between Voltage Sensors and Activation Gate in Voltage-gated K^+ Channels. J Gen Physiol 2002;120:663–676. [PubMed: 12407078]
27. Aggarwal SK, MacKinnon R. Contribution of the S4 segment to gating charge in the Shaker K+ channel. Neuron 1996;16:1169–1177. [PubMed: 8663993]
28. Seoh SA, Sigg D, Papazian DM, Bezanilla F. Voltage-sensing residues in the S2 and S4 segments of the Shaker K+ channel. Neuron 1996;16:1159–1167. [PubMed: 8663992]
29. Tempel BL, Papazian DM, Schwarz TL, Jan YN, Jan LY. Sequence of a probable potassium channel component encoded at Shaker locus of Drosophila. Science 1987;237:770–775. [PubMed: 2441471]
30. Soler-Llavina GJ, Chang TH, Swartz KJ. Functional interactions at the interface between voltage-sensing and pore domains in the Shaker K(v) channel. Neuron 2006;52:623–634. [PubMed: 17114047]
31. Swartz KJ, MacKinnon R. Hanatoxin modifies the gating of a voltage-dependent K+ channel through multiple binding sites. Neuron 1997a;18:665–673. [PubMed: 9136774]
32. Swartz KJ, MacKinnon R. Mapping the receptor site for hanatoxin, a gating modifier of voltage-dependent K+ channels. Neuron 1997b;18:675–682. [PubMed: 9136775]
33. Li-Smerin Y, Swartz KJ. Localization and molecular determinants of the hanatoxin receptors on the voltage-sensing domain of a K+ channel. J Gen Physiol 2000;115:673–684. [PubMed: 10828242]
34. Li-Smerin Y, Swartz KJ. Helical structure of the COOH terminus of S3 and its contribution to the gating modifier toxin receptor in voltage-gated ion channels. J Gen Physiol 2001;117:205–218. [PubMed: 11222625]

35. Lee HC, Wang JM, Swartz KJ. Interaction between extracellular Hanatoxin and the resting conformation of the voltage-sensor paddle in Kv channels. Neuron 2003;40:527–536. [PubMed: 14642277]

36. Phillips LR, et al. Voltage-sensor activation with a tarantula toxin as cargo. Nature 2005;436:857–860. [PubMed: 16094370]

37. Swartz KJ. Tarantula toxins interacting with voltage sensors in potassium channels. Toxicon 2007;49:213–230. [PubMed: 17097703]

38. Ruta V, MacKinnon R. Localization of the voltage-sensor toxin receptor on KvAP. Biochemistry 2004;43:10071–10079. [PubMed: 15287735]

39. Jung HJ, et al. Solution Structure and Lipid Membrane Partitioning of VSTx1, an Inhibitor of the KvAP Potassium Channel. Biochemistry 2005;44:6015–6023. [PubMed: 15835890]

40. Milescu M, et al. Tarantula toxins interact with voltage sensors within lipid membranes. J Gen Physiol. 2007(in review)

41. Lee AG. Lipid-protein interactions in biological membranes: a structural perspective. Biochim Biophys Acta 2003;1612:1–40. [PubMed: 12729927]

42. Lampe RA, et al. Isolation and pharmacological characterization of omega-grammotoxin SIA, a novel peptide inhibitor of neuronal voltage-sensitive calcium channel responses. Mol Pharmacol 1993;44:451–460. [PubMed: 8394998]

43. Lee CW, et al. Solution Structure and Functional Characterization of SGTx1, a Modifier of Kv2.1 Channel Gating(,). Biochemistry 2004;43:890–897. [PubMed: 14744131]

44. Herrington J, et al. Blockers of the delayed-rectifier potassium current in pancreatic beta-cells enhance glucose-dependent insulin secretion. Diabetes 2006;55:1034–1042. [PubMed: 16567526]

45. Papazian DM, et al. Electrostatic interactions of S4 voltage sensor in Shaker K+ channel. Neuron 1995;14:1293–1301. [PubMed: 7605638]

46. Long SB, Tao X, Campbell EB, MacKinnon R. Atomic structure of a Kv channel in a lipid membrane-like environment. Nature. 2007

47. Siemens J, et al. Spider toxins activate the capsaicin receptor to produce inflammatory pain. Nature 2006;444:208–212. [PubMed: 17093448]

48. Swartz KJ, MacKinnon R. An inhibitor of the Kv2.1 potassium channel isolated from the venom of a Chilean tarantula. Neuron 1995;15:941–949. [PubMed: 7576642]

49. Garcia ML, Garcia-Calvo M, Hidalgo P, Lee A, MacKinnon R. Purification and characterization of three inhibitors of voltage- dependent K+ channels from Leiurus quinquestriatus var. hebraeus venom. Biochemistry 1994;33:6834–6839. [PubMed: 8204618]

50. Hoshi T, Zagotta WN, Aldrich RW. Biophysical and molecular mechanisms of Shaker potassium channel inactivation. Science 1990;250:533–538. [PubMed: 2122519]

Acknowledgments

We thank Fabien Fontaine, Mark Mayer, Joe Mindell, Scott Ramsey, Shai Silberberg and members of the Swartz lab for helpful discussions, and the NINDS DNA sequencing facility for DNA sequencing. We thank Tetsuya Kitaguchi for cloning KvAP and Yasushi Okamura for generously providing Ci-VSP cDNA. This work was supported by the Intramural Research Program of the NINDS, NIH. A.A. Alabi was partially supported by the NIH Undergraduate Scholarship Program.

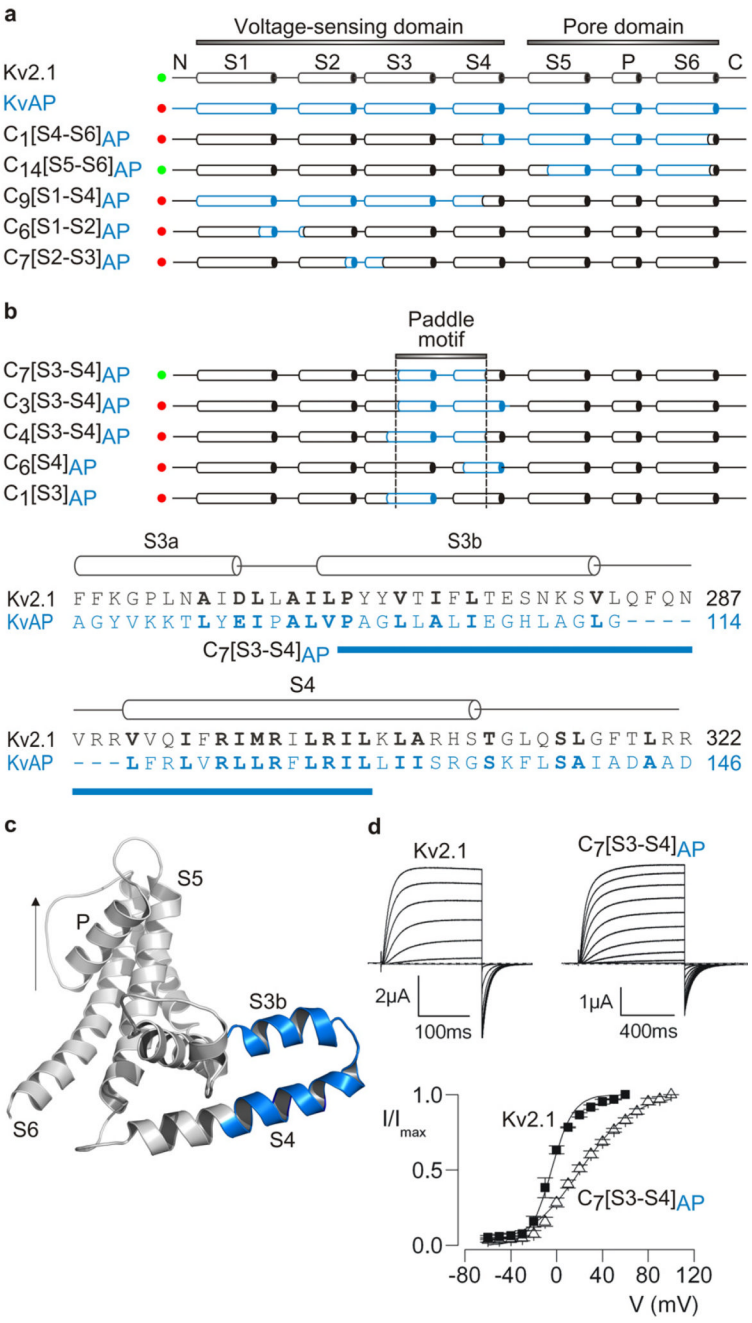

Figure 1. Transfer of the voltage-sensor paddle motif from KvAP to Kv2.1 channels

a, Overview of chimeras between KvAP (blue) and Kv2.1 (black). Constructs that result in functional Kv channel activity when expressed in oocytes are indicated with green circles and those that are non-functional are indicated with red circles. Chimera nomenclature is Cx[region transferred]donor channel, where x is the chimera number within that region. **b**, Defining the region within the voltage sensor of KvAP (indicated by dashed lines) that results in functional channels when transferred to Kv2.1. Alignment between KvAP and Kv2.1 in S3 through S4, highlighting (blue bar) the stretch of residues transferred to form C7[S3–S4]AP. Conserved residues are shown in bold lettering. **c**, Backbone fold of a single subunit from KvAP (PDB: 2A0L) (left) depicting the paddle region in blue. Arrow indicates the permeation pathway for

potassium ions. These and all subsequent structures were created using PyMOL (DeLano Scientific LLC). **d**, Potassium currents and tail current voltage-activation relations (n = 5–12; error bars are S.E.M.) for Kv2.1 and the C7[S3–S4]AP paddle chimera after expression in oocytes. Holding voltage was −80 mV and tail voltage was −60 mV.

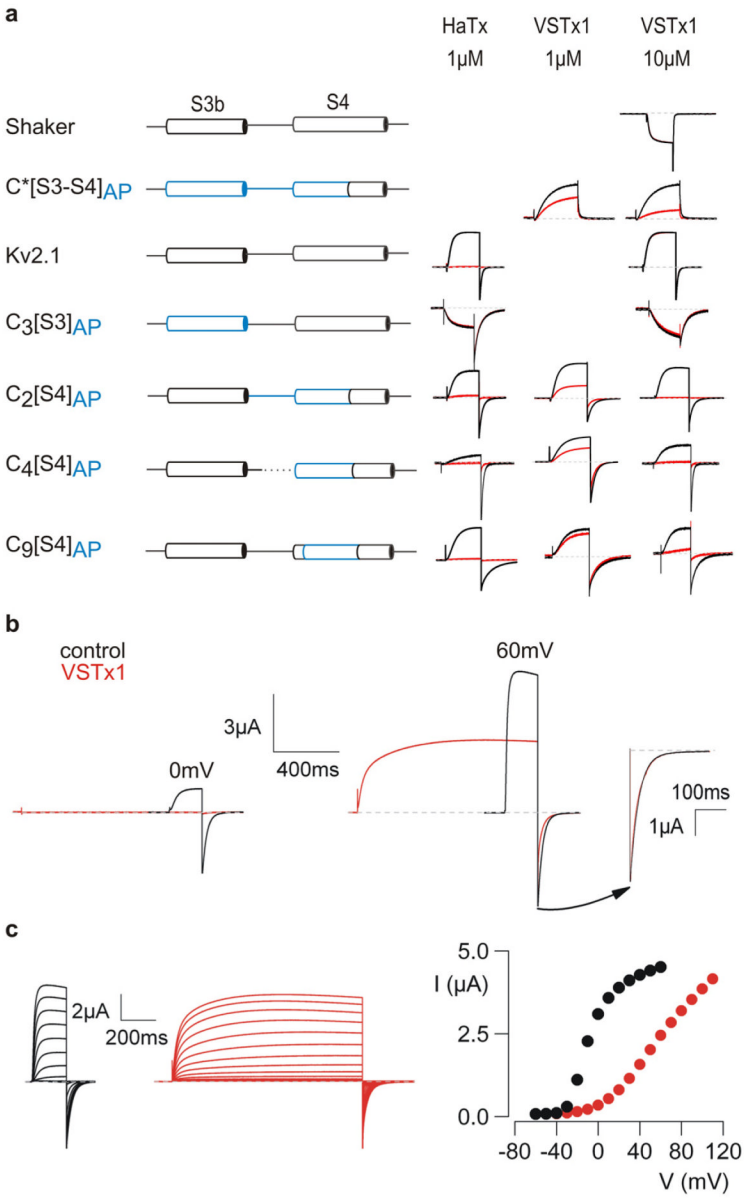

Figure 2. Sensitivity of KvAP paddle chimeras to extracellular tarantula toxins

a, Channel constructs, designated at the left with KvAP segments shown in blue, were expressed in oocytes and potassium currents elicited by depolarizations in the absence (black) or presence (red) of either HaTx or VSTx1. Depolarizations were to voltages near the foot of the voltage-activation relationship (relative open probability < 0.3) for each construct. All chimeras involving Kv2.1 are defined in Supplementary Fig 1. The paddle chimera in Shaker (C*[S3–S4]AP) was generated by transplanting P99–R126 of KvAP into P322–R371 of Shaker. C*[S3–S4]AP was studied with a low K^+ external solution and all others were studied with a high K^+ external solution (see Methods). Shaker has a very low sensitivity to HaTx [48] and was not studied. VSTx1-insensitive channels were only studied at the highest VSTx concentration. **b**, VSTx1 inhibition of chimera C2[S4]AP is voltage-dependent. Potassium currents were recorded for weak (0 mV, left) and strong (60 mV, right) depolarizations, before and after addition of 12 μM VSTx1. Inset to the far right shows scaled tail currents after

depolarization to 60 mV. **c**, Families of currents recorded in response to depolarizations in the absence (black) and presence of 12 μM VSTx1 (red). Holding voltage was −90 mV and tail voltage was −60 mV. Corresponding tail current voltage-activation relations for the traces shown, where tail current amplitude is plotted against test voltage.

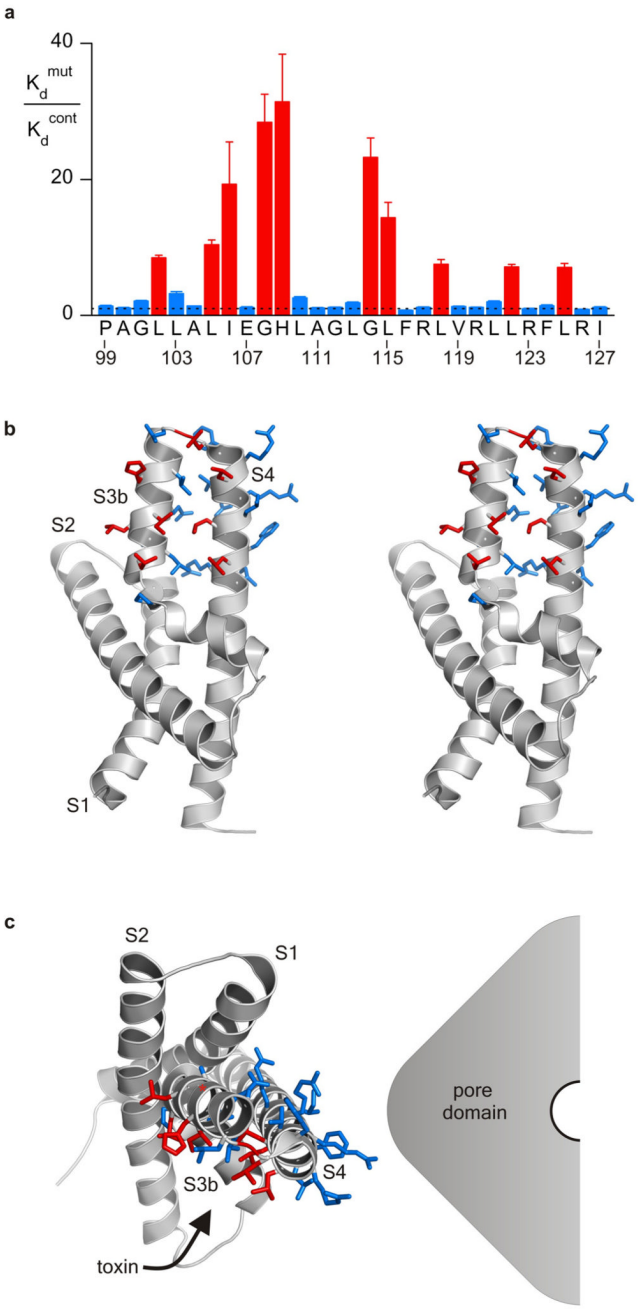

Figure 3. Structural analysis of the toxin-paddle interaction

a, Alanine scan of the paddle motif of KvAP in the C*[S3–S4]AP chimera where perturbations in apparent VSTx1 affinity (K_d^{mut}/K_d^{cont}) are plotted for individual Ala and Val mutants. The dashed line marks a value of 1 and numbering corresponds to the amino acid sequence of KvAP. Each mutant was initially examined using a concentration of toxin near the K_d for the control chimera; mutants displaying higher K_d values were further examined using higher toxin concentrations. n = 3–5 for each toxin concentration and error bars are S.E.M.. **b**, Stereo pair of the isolated voltage-sensing domain of KvAP (PDB: 1ORS) with side chains in the paddle colored according to perturbations in toxin affinity as in a. **c**, Positioning of the voltage-sensing

domain of KvAP adjacent to a hypothetical pore domain according to the X-ray structure of Kv1.2 (PDB: 2A79). The α-carbon of G108 is indicated by a red asterisk.

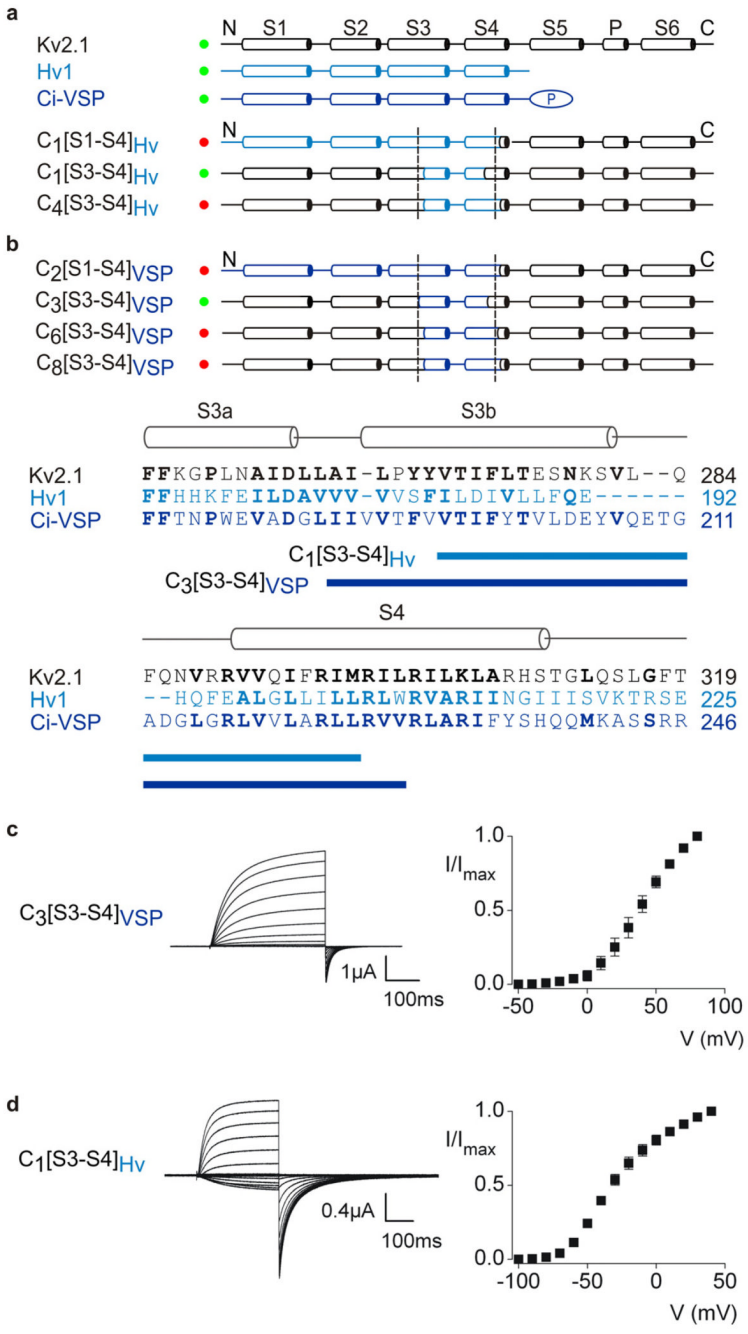

Figure 4. Transfer of the voltage-sensor paddle motif from Hv1 or Ci-VSP into Kv2.1 channels

Overview of chimeras between Hv1 (**a**, light blue), Ci-VSP (**b**, dark blue) and Kv2.1 (black). Constructs that result in functional Kv channel activity when expressed in oocytes are indicated with green circles and those that are non-functional are indicated with red circles. Dashed lines are the same as in Fig 1. The amino acid alignment shows the sequence of Kv2.1, Hv1 and Ci-VSP in S3 through S4, highlighting (blue bars) the stretch of residues transferred to form the two chimeras indicated. **c**, Current traces and tail current voltage-activation relations (n = 3; error bars are S.E.M.) for a chimera expressed in oocytes where the paddle of Ci-VSP was transferred into Kv2.1. Test depolarizations were to voltages between −50 and +80 mV, holding voltage was −80 mV and tail voltage was −50 mV. **d**, Current traces and tail current voltage-

activation relations (n = 3; error bars are S.E.M.) for a chimera where the paddle of Hv1 was transferred into Kv2.1. Test depolarizations were to voltages between −100 and +40 mV, holding voltage was −90 mV and tail voltage was −90 mV.

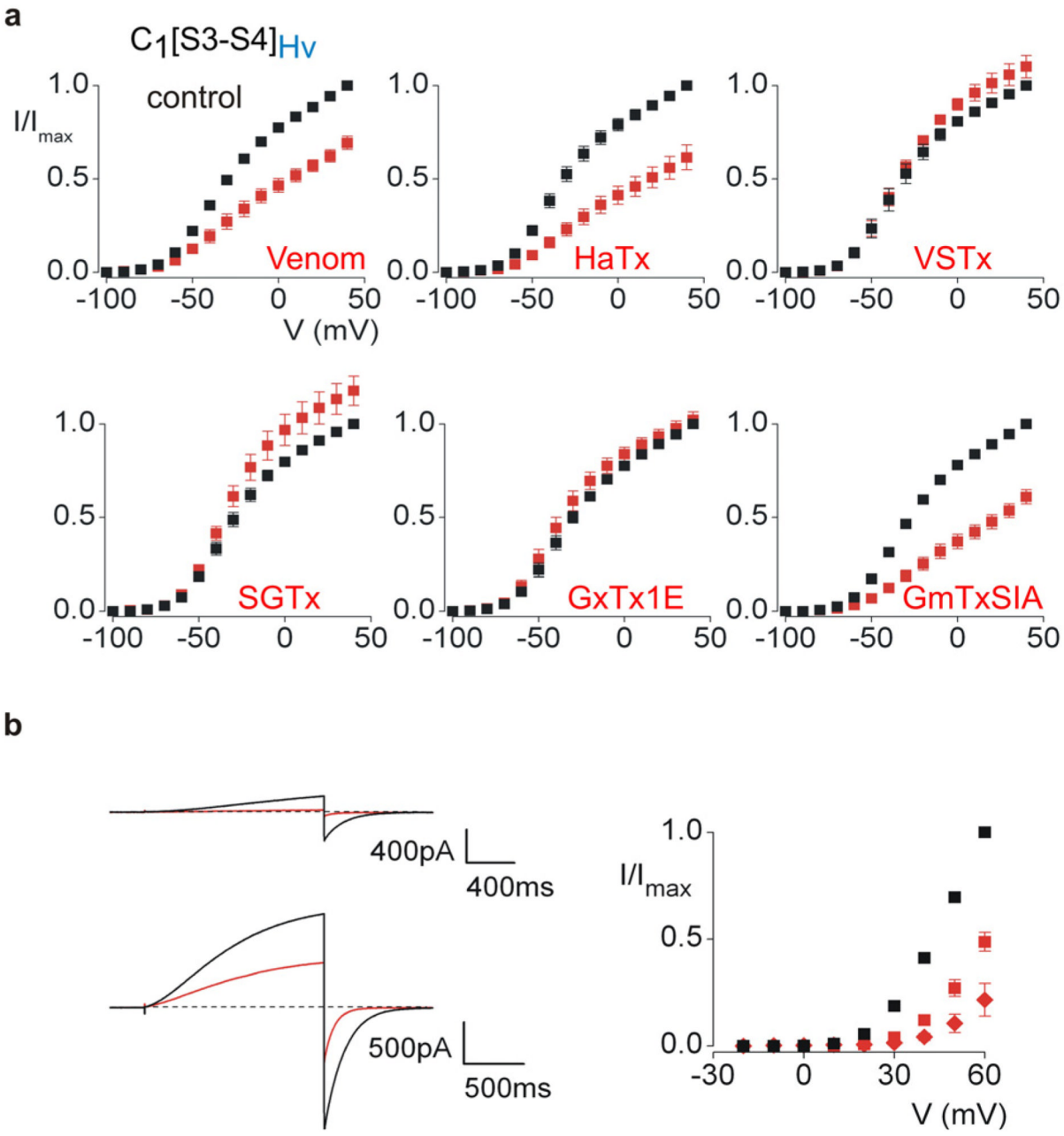

Figure 5. Sensitivity of a Hv1 paddle chimera and the Hv1 proton channel to tarantula toxins

a, Voltage-activation relations in the absence (black) and presence (red) of tarantula venom/toxins for a chimera containing the paddle of Hv1 in the Kv2.1 channel. Potassium currents were recorded using 300–500 ms test depolarizations from holding voltages between −100 and −90 mV, and tail voltages between −100 and −90 mV. Venom was applied at a 1:5000 dilution and toxin concentrations (in μM) were 2 for HaTx, 8 for VSTx1, 4 for SGTx1, 1 for GxTx1E and 10 for GmTxSIA. **b**, Proton currents recorded for Hv1 in response to weak (+30 mV; top) and strong (+60 mV; bottom) depolarizations, both in the absence (black) and presence (red) of 4 μM HaTx. Hv1 was expressed in HEK cells. Holding voltage was −40 mV and tail voltage was −60 mV. **b**, Tail current voltage-activation relations for Hv1 recorded in the absence

(black) and presence of 1 μM (red squares) or 4 μM (red diamonds) HaTx. For all voltage-activation relations n = 4–5 and error bars are S.E.M..

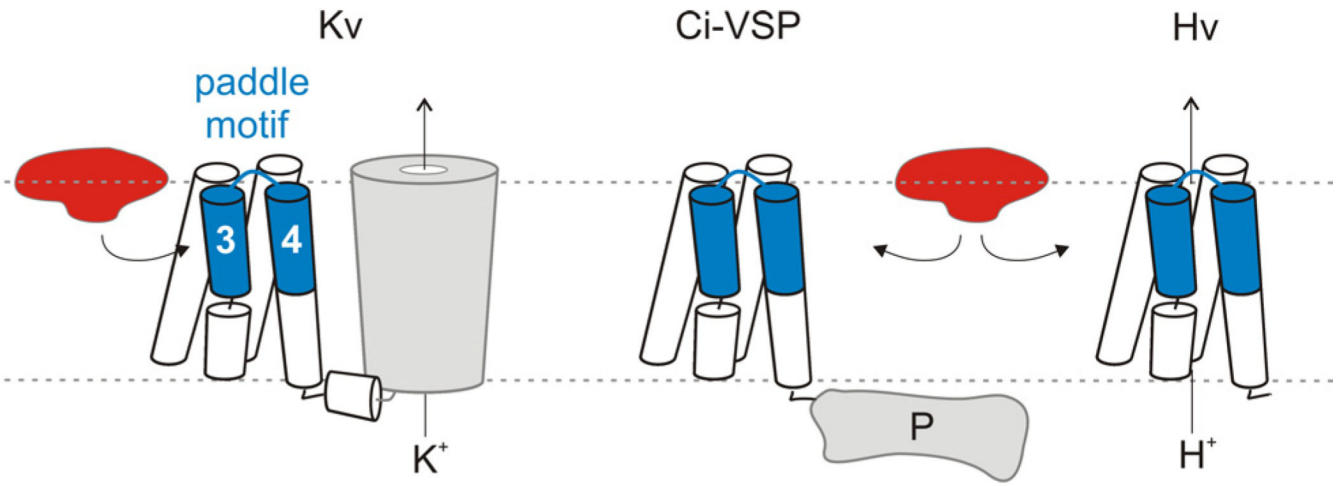

Figure 6. Tarantula toxins interacting with voltage-sensor paddle motifs

Cartoon depicting the interaction of tarantula toxins with voltage-sensor paddle motifs within the lipid membrane for Kv channels, and the voltage-sensing domain proteins, Ci-VSP and Hv1. Only one of the four voltage-sensing domains is shown surrounding the pore domain in Kv channels.